ISTITUTO NAZIONALE DI FISICA NUCLEARE

Sezione di Catania

INFN/TC–99/03
15 Febbraio 1999

INTEGRATED FRONT–END FOR A LARGE STRIP DETECTOR WITH E, ΔE AND POSITION MEASUREMENTS

N. Randazzo[(1),(2),] G.V. Russo[(2),(3)], C. Caligiore[(2),(4)], D. Lo Presti[(3)], C. Petta[(2),(3)], S. Reito[(2)], L. Todaro[(2)]; G. Fallica[(5)], G. Valvo[(5)]; M. Lattuada[(3),(6)], S. Romano[(6)], A. Tumino [(3),(6)]

1. Centro Siciliano di Fisica Nucleare e Struttura della Materia – Catania, Italy
2. Istituto Nazionale di Fisica Nucleare, Sezione di Catania, Italy
3. Dipartimento di Fisica, Università di Catania, Italy
4. now at STMicroelectronics – Catania, Italy
5. STMicroelectronics – Catania, Italy
6. Istituto Nazionale di Fisica Nucleare, Laboratorio Nazionale del Sud – Catania, Italy

Abstract

A large strip detector for position and energy measurement of heavy ions in a 100 MeV range has been realised. An improved version with an epitaxial thick layer for ΔE measurement is foreseen. This paper describes a charge preamplifier–shaper dedicated to an optimal use of the mentioned detector whose charge extracted will be holes. The dynamic range of 14 bit and 11 bit are expected for E and ΔE measurements, respectively.

Submitted to IEEE Transection on Nuclear Science

Published by ***SIS–Pubblicazioni***
Laboratori Nazionali di Frascati

1 Physical motivations

The renewed interest in molecule–like behaviour of nuclear matter came mainly from recent experimental results that support the theoretical predictions about the existence of very deformed cluster configurations, such as–chains [1],[2]. Experimental evidence has been found for a rotational band at high excitation energy in ^{16}O, with so large a moment of inertia as expected from a linear structure of four α–particles [1]. The rotational bandhead should be a 0+ level around 17 MeV of excitation energy, about 2 MeV above the threshold energy of dissociation into four α–particles. The existence of an elongated α–structure in ^{24}Mg is still a matter of investigation [2]; the excitation energy region around 46.4 MeV is seen as that of a rotational band with an intrinsic configuration of six α–particles in a chain.

Whenever, in consequence of a nuclear interaction, one of these α–structured levels, belonging to a self–conjugated 4n nuclei, is excited, mainly α–particles characterise the exit channel. The intermediate system can break up into α–particles directly or through a sequential decay into other self–conjugated 4n nuclei, which finally decay by emitting α–particles. As an example we can consider the decay of the hypothetical α–chain in ^{24}Mg at 46.4 MeV of excitation energy; one of the most important decays is into two ^{12}C excited at levels known to be characterised by a intrinsic configuration three α–particle; another possible decay is the three body channel $^{8}Be + ^{8}Be + ^{8}Be$, which can proceed through the formation of a 16O excited in correspondence to the 4α–chain region, and its subsequent decay into two correlated ^{8}Be. The experimental investigation of such configurations requires detection of α–particles in order to reconstruct kinematically the initial channels and all the correlations existing between the particles. Sometimes, when the experimental set–up does not allow the identification of detected particles, the presence of correlation between them could be powerfully used to provide for this lack. For example the relative energy spectrum of two coincident unidentified particles, which peaked at about 0.09 MeV, allows for identification of the emitting ^{8}Be ground state. In this particular case, the coincident detection of two α–particles has been sometimes performed [3] by using a Dual Position Sensitive Detector (DPSD), made of two Silicon Position Sensitive Detectors, assembled in close geometry. The mission angle and energy of ^{8}Be can be reconstructed by measuring the angles and energies of the two final α–particles, when each of them hits one half of such a DPSD.

When the reaction process involves nuclei decaying into more than two α–particles, a DPSD is not adequate and more fragmented detection systems are needed. The natural evolution of the DPSD is then a detector made of a number of parallel position sensitive strips. In this case detection efficiency is a function of the number of strips, for a given solid angle, and strongly depends on the multiplicity of the decay under investigation. Typical position and energy resolutions of commercial position sensitive detectors are better than 1%. In order to keep these features during the charge collection and signal formation, preamplifier noise better than 10 KeV should be desirable for both signals. This is particularly important for the position information which is deduced from a partition of the energy signal.

The kinematical identification still leaves a residual background in the reconstruction of the relative energy spectra of the α–particles, thus deteriorating the information on the parameters of the emitting state. ΔE–E identification of α–particles is then required in order to get complete information on the final state of the reaction.

A silicon ΔE layer around 10 μm thick was estimated to optimise both the identification of the emitted α–particles and the detection threshold for typical reactions performed at tandem

energies. Since the energy loss in transparent detectors is generally a small fraction of the total energy, its resolution does not affect heavily the total energy resolution. The main requirement is that its noise be low enough to allow for the separation of α–particles from the neighbouring light ejectiles in the ΔE–E plane. In consideration of the high capacitance of such a ΔE detector, electronic noise of few tens of KeV should still be enough to maintain the overall characteristics of this telescope suitable for the class of experiments above described.

2 Detector design

While the Energy–Position detector has been produced by STMicroelectronics in its Catania R&D department, instead the ΔE–Energy–Position is yet under developement.

A cross section of the Energy–Position detector is shown in Fig.1. The total area is 5 x 50 mm^2, while the sensitive area of the strip is 3.1 x 48 mm^2.

The detector capacitance is about 32 pF.

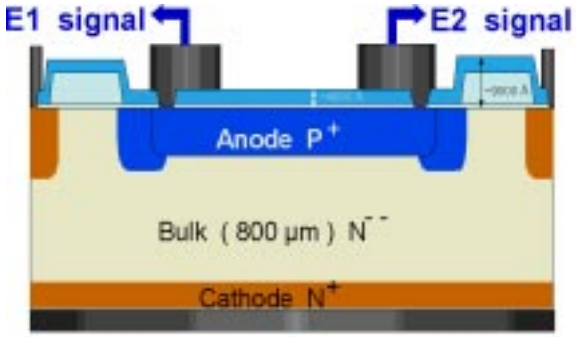

Fig. 1 – Cross section of the Energy–Position detector (not in scale).

Fig. 2 – Structure of the Energy–Position detector (not in scale).

The detector has the structure of a PIN diode (see Fig.2). The anode is obtained by ion implantation of boron on the front of an n–type FZ <111> wafer of very high resistivity ($\rho > 9000\ \Omega\cdot cm$), with a thickness of 800 µm. At both extremities of this implanted P strip there are two readout contacts (DC coupled). The position information (only in one direction) is deduced from a partition of the energy signal, extracted from these two contacts. The anode is surrounded by a P^- ring, which prevents the edge of the junction from local breakdown phenomena. Near the edge of the entire detector there is a channel stopper, obtained by ion

implantation of a high dose of phosphorus. On the back of the detector, the cathode is formed by an NN^+ pseudo–junction that acts as a non–injecting ohmic contact. The upper anode is the entrance window of the detector. Therefore, the superficial layer above the depleted region must be as thin as possible in order to avoid absorption of radiation and energy straggling. For this reason, the anode is formed by an ultra thin implanted boron layer with only a 0.4 μm oxide film above it. The metal layer (Ti/W + Al/Ti) does not cover the entire sensitive area, but there are only two bonding pads over the readout contacts. These contacts are 10 μm large rectangles as close as possible to the extremities of the P strip. Because of the high thickness of the wafer, this detector has a full depletion voltage of 165 ÷ 180 Volts. The mean leakage current at full depletion is ~200 nA. The charge collected by the anodes is composed by holes.

A more complex double face detector is now in course of development at STMicroelectronics. This new detector will be a monolithic telescope having four contacts: on the front there will be the ground contact and the ΔE readout; on the back will be two Energy–Position readout contacts at the extremities of a resistive rear layer.

In this new telescope the ΔE and the E stages will be two reverse biased diodes working at full depletion. The ΔE stage will be ~10 μm thick and will work at an operating voltage of ~50 Volts; the E stage, as in the previous detector, will be 800 μm thick and will work at ~180 Volts. The detector capacitance of the ΔE stage is foreseen as about 1000 pF.

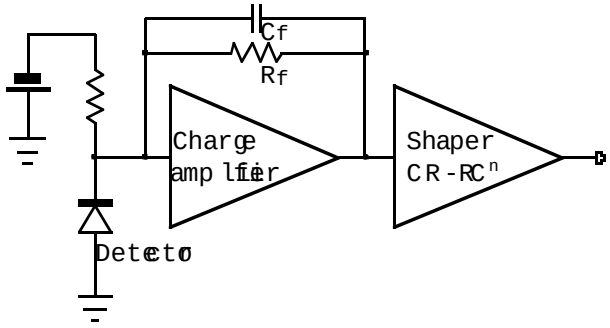

Fig. 3 – The read–out system for solid state detectors.

3 Front–End for solid state detectors

To measure the energy lost by a particle in a detector a readout system must be made. Fig.3 shows a schematic drawing of the front–end for solid state detectors. A charge preamplifier gives a signal whose amplitude is proportional to the energy losses. A filter reduces noise to give a better resolution.

In the case of Intermediate Energy Physics Experiments (IEPE) the limited number of channels has led to the use of expensive modular devices both for preamplifiers and filters [4]. Nevertheless new more complex experiments require a number of channels comparable to those of High Energy Physics Experiments (HEPE) [5]. At first physics have adopted hybrid or SMD circuits [6]. More recently monolithic front–end devices suitable for IEPE use have been presented [7],[8].

Four main advantages can be achieved with a monolithic device. The first one refers to the power dissipation that can be decreased by up to three orders of magnitude compared with modules and up to two orders of magnitude in respect of hybrids. The second is the cost of the electronic chain that decreases very much both for amplifiers and power supplies. The size of a

monolithic device is very small compared with other solutions. As a consequence one can make a very fine segmentation of multidetector systems. The last advantage is that a monolithic preamplifier–shaper is designed taking into account its specific application. Therefore its performances can be better that general purpose modules or hybrid solutions.

The resolution properties of a readout system depend mainly on the leakage current and the capacitance of the detector. One can reach appreciable results using an appropriate preamplifier. Its input transistor is the most important device of the whole chain [9]. In the case of very large area detectors, as in IEPE, the capacitive coupling between detector and preamplifier requires a very large area transistor really unusual in integrated technologies [8]. Nevertheless it is convenient to design a dedicated ASIC preamplifier–shaper, that with several remarkable advantages, gives very good results in the presence of a specified detector.

We have adopted a semigaussian RC–CR^2 filter [10]. To reduce costs and sizes further the filter has been implemented in a single chip. We have chosen a solution that gives very good results also if we compare them with both module and hybrid solutions.

The transfer function of this type of filters can be written as:

$$F(s) = k \frac{s/\tau^n}{(s+1/\tau)^{n+1}} = k \frac{\omega_o{}^n s}{(s+\omega_o)^{n+1}} \qquad (1)$$

4 The design

The main characteristics of the readout are energy resolution and dynamic range. The first depends on the noise properties of the system but, as for the reason that will be explained in the next section the sensitivity of the preamplifier can play a great role especially for low capacitance at low sensitivity. And this is the case in the present application. Our design start from noise considerations, but they are strictly connected with dynamic range.

4.1 Noise considerations

In a readout system the overall noise is obtained taking into account the contribution of the preamplifier and the effect of the shaper. Generally speaking one attributes the source of noise to the preamplifier while the shaper is used to decrease it with a filtering action. Nevertheless the shaper is not an ideal object. It has its own intrinsic noise. Its behaviour can be retained ideal only when its contribution is negligible in respect of the total noise. A good shaper having an amplification of 1÷2 V/V has an intrinsic noise of a few hundreds of microvolts. Preamplifiers having a sensitivity of more then 100 mV/MeV have intrinsic noise of about 1 mV. In Low and Intermediate Energy Physics applications one needs very high dynamic ranges, see 13–15 bit. Using standard integrated technologies it is not possible to achieve such a high sensitivity in the preamplifier stage. It is difficult to exceed more than 10 mV/MeV. Then one has low noise in the preamplifier stage and so the contribution of both the shaper and the biasing system is no longer negligible. This problem is more consistent for detectors having low capacitances. This behaviour will be confirmed with our measurements. In our design we have taken a special care in the design both of the preamplifier and of the filter to achieve an overall minimum noise. We have applied the standard techniques of a low noise amplifier to limit its effect on the shaper. For the preamplifier we have used the optimisation procedure described below.

4.2 The first transistor

The main source of noise for the whole chain is the first transistor of the first stage. Preamplifier noise depends both on its design and process parameters. Our devices, named OSCAR, have been designed in CMOS 1.2 μm, double–poly, double–metal process. We have investigated all the contributions of noise: flicker (ENC_f), thermal (ENC_t) and shot (ENC_s). The analysis has been performed as in previous papers [8]. We have assigned some parameters as, for instance, the leakage current ILk, the capacitance Cd of the detector, the range of the shaping time $\tau s = n.\tau$, according to ADC and rate restrictions, the number n of the integrators and an appropriate range for the drain current ID of the first transistor.

Assuming an ideal shaper, for a readout system such as that shown in Fig.3 one has [11]:

$$\left.\begin{aligned} ENC_f^2 &= \frac{Kf}{C_{ox}^2 WL}\ \frac{C_t^2}{q^2\ 2n}\ fn \\ ENC_t^2 &= \frac{8}{3}\ KT\ \frac{1}{gm}\ \frac{C_t^2\ B\ (1.5, n\ -\ 0.5)\ n}{q^2\ 4\pi\ t_s}\ fn \\ ENC_S^2 &= 2\ q\ ILK\ \frac{t_S\ B\ (0.5, n\ +\ 0.5)}{q^2\ 4\pi\ n}\ fn\ . \end{aligned}\right\} \qquad (2)$$

Kf is the flicker coefficient of the first NMOS transistor; Cox is the specific oxide capacitance of its gate, W, L are its sizes, Ct = Cd + Ci + Cf + Cp is the sum of the detector capacitance, the input transistor capacitance, the feedback capacitance and the parasitic capacitances at the input gate. The trasconductance of the first transistor is gm. K is the Boltzman constant, q is the electron charge, T is the absolute temperature, B is the Beta function

$$B\ (p,\ q)\ =\ \int_0^1\ t^{p-1}\ (1-x)^{q-1}\ dx,$$

and

$$fn\ =\ \left(\frac{n!^2\, e^{2n}}{n^{2n}}\right).$$

The total noise ENC_{tot}, is given by:

$$ENC_{tot}\ =\ \sqrt{ENC_f^2\ +\ ENC_t^2\ +\ ENC_S^2}\,. \qquad (3)$$

4.3 Noise optimisation

We have used a folded cascode solution for the charge preamplifier since the simple cascode amplifier has a good amplification but a limited common mode input range. This limitation is overcome using the folded cascode solution. Its gain $A0 = gm \cdot Ro$ depends on the trasconductance gm of the first transistor, that in turn, depends on its drain current. Ro is its very high output impedance [12].

The output of the preamplifier of the Energy channel is used to generate a signal for timing too. A rise time of not more than 50 ns is required. Since the latter, and therefore the bandwidth, depends on ID we have established the need to search for the optimum conditions for noise in an ID range according to this bandwidth requirement and power dissipation

limitations.

To optimise the Energy channel performances we have taken into account the leakage current and the capacitance of the detector. A reasonable choice of the filter order must also be made. The order of the filter, generally speacking, ameliorates noise. But this is not really true in every case. As we have already said in Sect. 4.1, when the preamplifier sensitivity is very low, the theoretical improvement of noise due to a bigger order is lost by the worsening of intrinsic shaper noise due to the included devices. For this reason we have limited the order of the filter to n = 2.

To minimise noise, the detector and the input transistor must be appoximately capacitively matched. If we can neglect $C_f + C_p$ then $C_t \approx 2 \cdot C_d \approx 2 \cdot C_i \approx 2 \cdot C_{ox} \cdot W \cdot L$. The technological process chosen determines the $W \cdot L$ product. Then the expressions (2) can be condensed as:

$$\left.\begin{array}{l} ENC_f^2 \approx \alpha \; I_D^{AF-1} \\ ENC_t^2 \approx a \; L \cdot t_s^{-1} \cdot I_D^{-1/2} \; \alpha \; W^{-1} \cdot t_s^{-1} \cdot I_D^{-1/2} \\ ENC_s^2 \; \alpha \; I_{LK} \cdot t_s \; . \end{array}\right\} \qquad (4)$$

AF is the SPICE coefficient of the Flicker noise.

To reduce thermal noise a minimum L of the first transistor must be utilised. W is a direct consequence of this choice. The choice of the shaping time ts is a compromise between thermal and shot noise. In an analogous way I_D is a compromise between flicker, thermal noise and power dissipation.

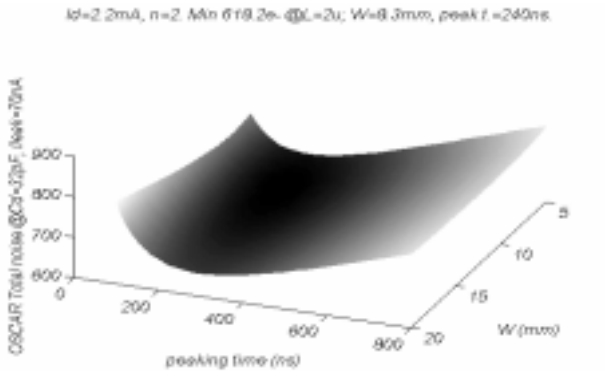

Fig. 4 – Energy channel preamplifier optimisation.

The above expressions have been manipulated by a code capable of optimising noise vs. I_D, W and ts. We have assumed an upgraded leakage current I_{Lk} = 70 nA. The result is depicted in Fig.4 in the case of n =2 and Cd = 32 pF.

Using an ideal shaper with zero intrinsic noise a minimum noise of 618 e^- has been calculated at I_D = 2.2 mA, using a NMOS transistor with L = 2 μ e W = 8.3 mm. The peaking time must be about 240 ns. At Cd = 0 pF and I_{Lk} = 0 nA we have calculated about 175 e^- rms while at Cd = 32 pF and I_{Lk} = 70 nA we have calculated about 618 e^- rms. These results are summarized in the 3rd÷4th columns of TABLE I.

TABLE I		OSCAR E channel calculated noise			
		Optimised		OSCAR	
W (mm)		8.3		10	
ts (ns)		240		700	
Cd (pF)		0	32	0	32
Ilk (nA)	0	175	510	160	338
	70	410	618	692	772

An analogous optimisation for the ΔE channel (Cd = 1000 pF, I_{Lk} = 10 nA), using about the same drain current I_D = 2.2 mA leads to the results depicted in Fig.5. A minimum noise of 2150 e^- rms could be achieved if W = 38.4 cm! A transistor with this size is absolutely not realistic!

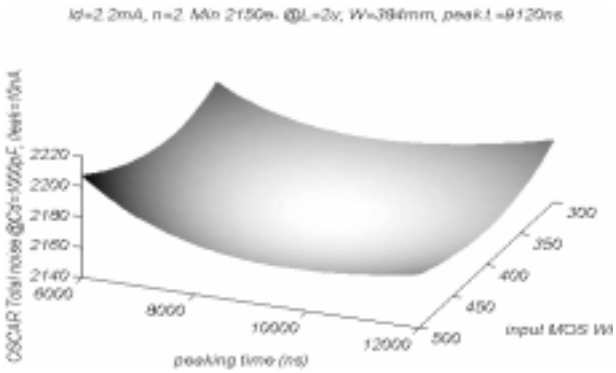

Fig. 5 – ΔE channel preamplifier optimization.

Instead of designing two different preamplifier–shapers we have decided to adopt a compromise and to make a single solution which is acceptable for both E and ΔE measurements. Since the most pressing assignment as regards resolution was for E measurement the transistor width was fixed at 10 mm. This is a very good choice for E measurement. Nevertheless the peaking time was enlarged up to 700 ns. The latter solution, is a compromise with the need for resolution for E or ΔE measurements. Increasing the peaking time too much will compromise the E resolution while it ameliorates the ΔE resolution. Because of the rate it is not recommended to enlarge τs to much. A peaking time too short could cause difficulties to the ADC that requires a minimum peaking time of 500 ns.

Using an ideal shaper with zero intrinsic noise at Cd = 0 pF and I_{Lk} = 0 nA we have calculated about 160 e^- rms while at Cd = 32 pF and I_{Lk} = 70 nA we have calculated about 772 e^- rms (see the 5rd–6th columns ot table I).

Both calculated thermal and flicker noise are shown in Fig.6. The calculated effect of shot noise is shown in Fig.7.

For ΔE measurement we have calculated about 8640 e^- rms, at Cd = 1000 pF and I_{Lk} = 10 nA.

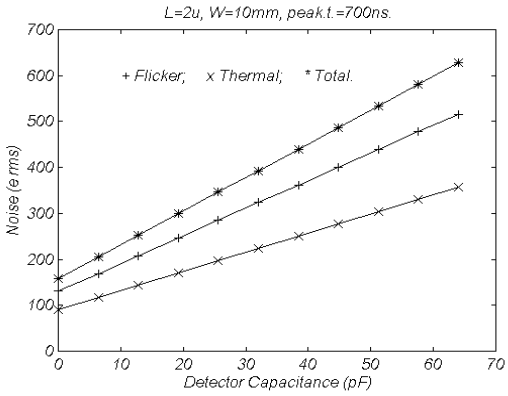

Fig. 6 – E channel calculated thermal

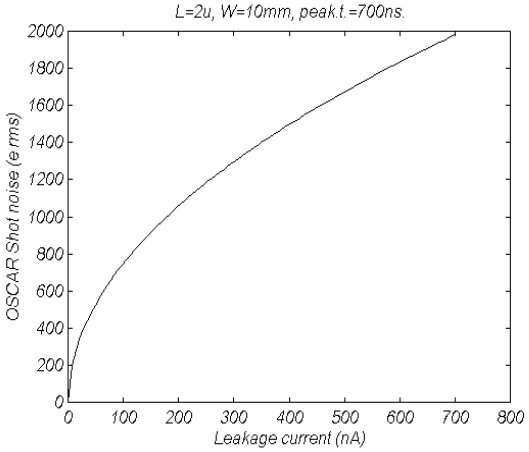

Fig. 7 – Preamplifier shot noise.

4.4 Preamplifier design

The preamplifier stage shown in Fig.8 is based on a single–ended folded cascode. Two very important features of the folded cascode are that the dominant pole is established by the capacitance at the output node and that the slew rate depends both on this capacitance and the biasing current. This solution offers better performances in terms of stability and gain compared with the standard cascode [12].

Taking into account that the detector drains positive charges the preamplifier was designed to achieve the best dynamic.

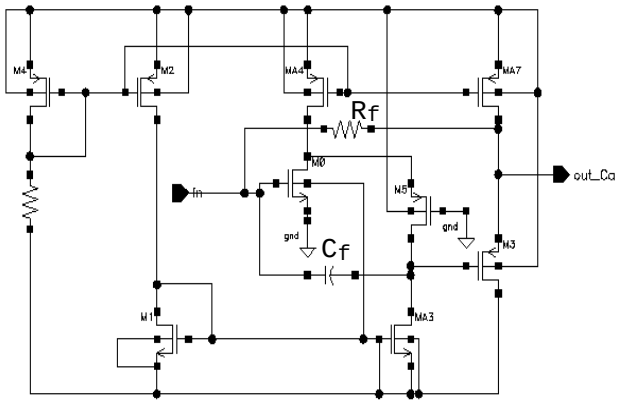

Fig. 8 – Preamplifier schematic diagram.

Let us call Cf and Rf the feedback group. The transfer function of the preamplifier is [11]

$$\frac{V_{out}}{I_{in}} = \frac{g_m}{g_m / R_f + s g_m C_f + s^2 C_t (C_f + C_L)}. \quad (5)$$

The output signal caused by a charge Q in the detector is:

$$V_{out}(t) = \frac{Q \tau_1}{C_f (\tau_1 - \tau_2)} \left(e^{-t/\tau_1} - e^{-t/\tau_2}\right) \quad (6)$$

where $\tau_1 = R_f C_f$ and $\tau_2 = C_t(C_f + C_L)/g_m C_f$. If $\tau 1 >> \tau 2$ the speed of the preamplifier depends on $\tau 2$. If this is the case, the rise time is:

$$tr = 2.2\ Ct\ (Cf + CL) / gmCf \qquad (7)$$

The NMOS input transistor at I_D = 2.2 mA gives gm = 37 mA/V. The choice of a very high value for the external feedback resistance (Rf = 10 MΩ) is to decrease significantly the parallel noise. It is not convenient to integrate a resistor of such a high value.

We have used an internal total feedback capacitance Cf = 4.4 pF to obtain a sensitivity of the preamplifier 10 mV/MeV or 223 μV/fC. When Cd = 32 pF, $\tau 1 >> \tau 2$. Using the expression (7), in this condition and with CL = 20 pF, we have calculated a rise time tr = 21 ns.

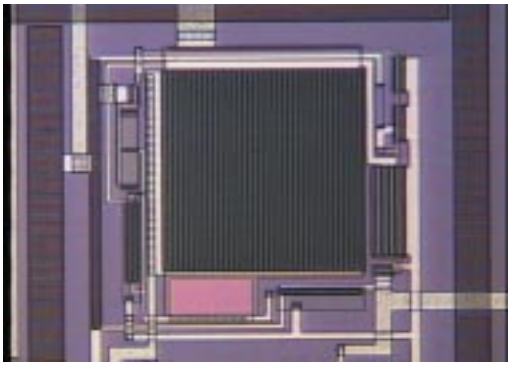

Fig. 9 – First transistor gate and feedback capacitance

Special care was taken to obtain an overall Cf = 4.4 pF. To achieve this value a slightly smaller Cf capacitor was designed with the intenion of compensating the effect of parasitic, pad, resistor bonding, pin and case capacitances. To control better parasitic capacitance and to save silicon area Cf is obtained extending the first transistor gate. Fig.9 shows the first transistor gate and the feedback capacitance Cf.

The unusual dimension of the first transistors (10.000/2) has imposed the need of special care in its design. To limit extra noise due to the high resistivity of the bulk the latter was polarised around the first interdigited transistor using a special layout technique.

We have used only one power supply for the input transistor to decrease its power dissipation. In fact it does not exceed 760 μW. Taking into account the remaining part of the preamplifier, the overall power dissipation without the shaper is less than 2.8 mW, that is at least 50 times smaller than hybrid modules.

4.5 Shaper design

The shaper has been implemented in the same chip like a CR–RC^2 with a simple CR passive filter and two bilinear active filters. The latter use double–stage Miller–compensated Full–Custom operational amplifiers. The power dissipation is about 3.3 mW. Driving capability of an external CL = 20 pF is provided. The output linear dynamic range allowed by the technology is 2 V. To obtain a dynamic range of 120 MeV the overall sensitivity must be 2/120 V/MeV = 16.6mV/MeV. Since the preamplifier sensitivity is 10 mV/MeV the shaper must have

As0 gain of up to 1.66 V/V. The transfer function is given by (1). Since $\tau p = 700$ ns and $n = 2$, we have $\tau p = 2\tau = 2/\omega 0 = 1/\pi f0$. Then $f0 = 1/\pi\tau p = 455$ KHz. As0, n and f0 was used to design the filter.

4.6 OSCAR layout

The picture of OSCAR is shown in Fig.10. You can see six equal channels. This means that one chip is dedicated to two strips. Provision is made for channel testing. To limit crosstalk between the channels an accurate guard ring was inserted. To measure crosstalk, two test capacitors are put in, connecting together odd or even channels. Power supply is ±2.75V. The size of OSCAR is 2 x 4 mm2.

5 Measurements

A set of accurate measurements was made. The most important are given below.

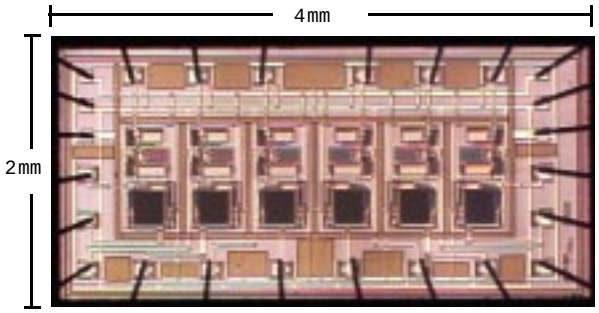

Fig. 10 – Oscar photo.

5.1 Sensitivity measurements

We have measured the preamplifier output to 3 MeV using a sampling Scope Tektronix TDS 753D. The result is shown in Fig.11. The step is about 28.96 mV. Then the sensitivity of the preamplifier is about 9.65 mV/Mev.

The output response of the Preamplifier–Shaper to 2 MeV is shown in Fig.12. A voltage of 31.6 mV has been measured and the overall sensitivity is about 15.8 mV/Mev or 352 μV/fC. Then the shaper amplification As0 is about 1.64 V/V. The output range is 2 V corresponding to a 126 MeV range.

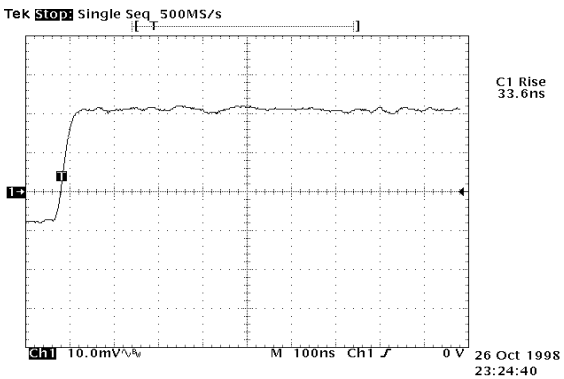

Fig. 11 – Preamplifier measured 3 MeV response.

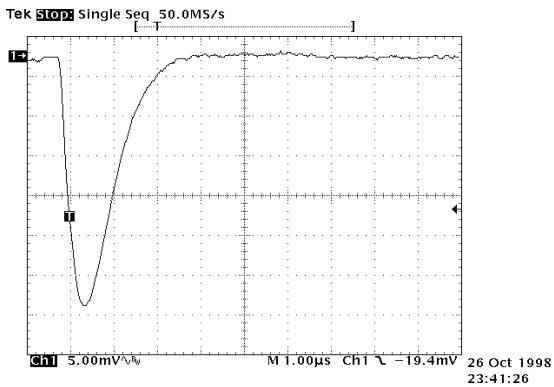

Fig. 12 – 2 MeV measured overall response.

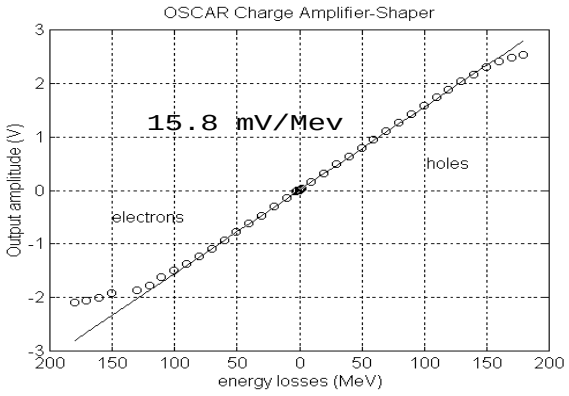

Fig. 13 – Preamplifier/shaper linearity.

5.2 Timing measurements

From Fig.11 you can see that the preamplifier rise time is about 34 ns. This is a very good performance for timing! Taking into account the loading effect of the scope (about 8 pF) this result agrees with the theoretical prediction of Sect. 4.4.

The peaking time that we have measured from Fig.12 is about 670 ns, very close to the desired value of 700 ns.

5.3 Transfer function measurement

We have measured the overall transfer function using the 3 GHz Network Analyser HP8753D. $\omega o \approx 3$. Mrad/sec. The peaking time = $n/\omega o$ is confirmed as 670 ns.

5.4 Linearity measurement

The linearity of the preamplifier is very good, as you can see from its measurement given in Fig.13. We have obtained better than ±.5% for electrons up to 60 MeV and up to 130 MeV for holes.

5.5 Noise measurements

We have measured OSCAR noise both for E and ΔE use. In Fig.14 the dotted points represent the result of our measurements.

At Ci = 32 pF and $I_{Lk} = 0$ the total noise is about 3360 e^- rms, that is 12.1 KeV. Then, in absence of leakage current we have a dynamic range of 126 MeV/12.1 KeV, that is 10413. More than 13 bit! Shot noise depends on the square root of leakage current. That is ENCs = $k \cdot I_{lk}^{1/}2$. From Fig.7 we can calculate the k value for OSCAR as about 75 when Leakage current is expressed in nA. If we want 13 bit of dynamic range, for E measurement, the total noise can increase up to 126 MeV/8192 = 15.38 KeV. Then, at Cd = 32 pF, shot noise can be up to $(15.38^2 - 12.1^2)^{1/2}$ KeV = 9.49 KeV; that is 2630 e^-. In conclusion the maximum allowable leakage current is $(2630/75)^2$ nA = 1.23 mA.

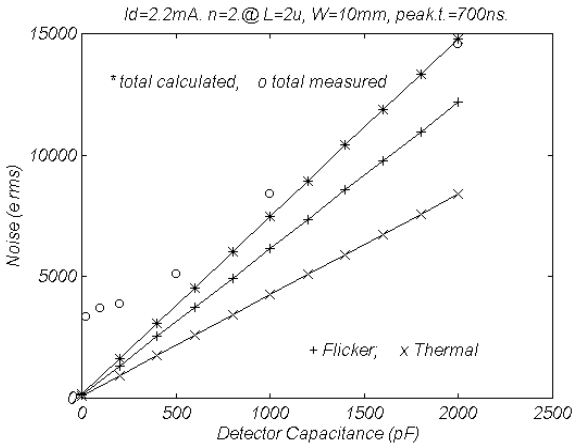

Fig. 14 – Measured and calculated noise.

At Ci = 1000 pF and ILk = 0 the total noise is about 8115 e- rms, that is 30.4 KeV. So, in absence of leakage current we could have a dynamic range of 126 MeV/30.4 KeV, that is 4144: 12 bit.! Nevertheless in the case of ΔE measurement using the detector of Fig.1 in our experiments the expected input dynamic will be not more than 20 MeV. then the true dynamic range, in this case is about 20 MeV/ 30.4 KeV = 656 that means more than 9 bit.

In any case the experimental requirements for noise are largely satisfied.

In the same Fig.14 the measured values are compared with the calculated ones. The great difference for E measurements, that is for small detector capacitances, was predicted in Sect. 4.1.

We have measured an intrinsic shaper noise of about 140 μV (8.86 KeV because of 15.8 mV/MeV of sensitivity). Referring to the shaper input (AV0 = 1.64) we have about 85 μV. If, for instance, the output dynamics could be 10 V, instead of only 2 Volt, as in the case of the ORTEC 542 shaper, with the same range 126 MeV/10 V 140 μV corresponds to only 1.77 KeV, instead of 8.86 KeV.

5.6 Crosstalk measurements

Crosstalk simulation between adjacent channels has given more than 12o dB. Applying a 100 MeV impulse 100 dB minimum is guaranted.

6 Conclusions

The main objectives of the OSCAR preamplifier have been achieved. Sensitivity, dynamic range, noise, linearity and power dissipation satisfy the assigned conditions for the experiment foreseen.

The most important characteristics of this realisation are the good performances compared with low cost, dissipation and size that render this device appreciable in IEPE especially when the number of channels is very high.

From the final considerations of Sect.5.5 one must make a general consideration about the choice of technology, the sensitivity and noise performances. Using a high voltage technology for the shaper, one could achieve a higher sensitivity, and, of course, a better overall noise. This is the main suggestion of this work!

Acknowledgement

We gratefully acknowledge C. Calì, P. Litrico, N. Giudice, S. Urso for collaboration.

References

[1] M. Freer et al, Phys. Rev. C 51, 1682 (1995).

[2] A. H. Wuosmaa, Z. Phys. A349, 249 (1994);
S. P. G. Chappell et al, Phys. Rev. C51, 695 (1995);
R. A. Le Marechal et al, Phys. Rev. C 55, 1881 (1997);

[3] M. Aliotta et al, Z. Phys. A 354 ,119 (1996);
M. Lattuada et al, Il Nuovo Cimento A110, 1007 (1997).

[4] EG&G Ortec, Model 122X Preamplifier Op. & serv. Manuale, Oak Ridge, USA
EG&G Ortec, Modular Pulse Processing Electronics and Semiconductor Radiation Detector, 1997

[5] S. Aiello et al – Nucl. Phy. A, Vol. A583, p. 461, 1995
E.Costanzo, M.Lattuata, D.Viciguerra – Private communication

[6] CAEN, Model A422, Charge Sensitive Hybrid Pre–Amplifier, Preliminary Data Sheet, (1993)
CEA Saclay – Preampli 588, 1993
CEA Saclay – DAPNIA/SEI, Groupe Electronique Analogique, Preamplicateur de Charg Type Chimera, (1995)
eV Products, Single Channe Preamplifier Hybrid Circuits eV–5091/92/93/94, (1992) Saxsonburg, PA, USA

[7] V. Re, Private Communication, (1993)

[8] N.Randazzo, G.V.Russo, D.LoPresti, S.Panebianco, C.Petta, S.Reito, IEEE Tr. Nucl. Sc., Vol.44, (1997), 31
N. Randazzo, G. V. Russo, et al, Low Power – Low Noise, Integrated Preamplifier–Shaper for Large Area Silicon Detectors – to be published by Nucl. Instr. & Meth.

[9] E. Gatti, P. F. Manfredi, Riv. Nuovo. Cim., Vol. 9, n° 1, p. 1, (1986)

[10] E.Baldingen, W.Franzen, Advances in Electronics and Electron Physics, Academic Press (1956)
V.Radeka, Nucl. Instr. & Meth., A266, (1984), 209

[11] Z. Y. Chang, W. M. C. Sansen – Low–Noise Wide–Band Amplifiers in Bipolar and CMOS Technologies – Boston – Kluwer Academic Publisher, 1991

[12] A.S.Sedra, K.C.Smith Microelectronic circuits, 1998, Oxfors Un. Press.
G. U. Ismail, H. Fiez – Analog VLSI – Mc Graw Hill– 1994